RSC Advances

This is an *Accepted Manuscript*, which has been through the Royal Society of Chemistry peer review process and has been accepted for publication.

Accepted Manuscripts are published online shortly after acceptance, before technical editing, formatting and proof reading. Using this free service, authors can make their results available to the community, in citable form, before we publish the edited article. This *Accepted Manuscript* will be replaced by the edited, formatted and paginated article as soon as this is available.

You can find more information about *Accepted Manuscripts* in the Information for Authors.

Please note that technical editing may introduce minor changes to the text and/or graphics, which may alter content. The journal's standard Terms & Conditions and the Ethical guidelines still apply. In no event shall the Royal Society of Chemistry be held responsible for any errors or omissions in this *Accepted Manuscript* or any consequences arising from the use of any information it contains.

ROYAL SOCIETY OF CHEMISTRY

www.rsc.org/advances

Multifunctional Particle Coating by Plasma Process and its Application to Pollution Control

Anna Nasonova[1] and Kyo-Seon Kim[*]

Department of Chemical Engineering, Kangwon National University
Chuncheon, Kangwon-Do, Republic of Korea

ABSTRACT

Multifunctional particle coating by Plasma-Enhanced Chemical Vapor Deposition (PECVD) and its application are presented in this review. A rotating PECVD reactor can be used to prepare a single-layer or multi-layer thin films on substrate particles of various materials with different shapes by using various gas/liquid precursors. The current development of the rotating PECVD process for particle coating of high quality is discussed, along with simulation and experimental results, in the present review. Flexibility in changing the process variables of rotating PECVD enables this process to be considered as a promising method for particle coating with possible applications in many different fields.

* Corresponding author. Tel: +82-33-250-6334, E-mail: kkyoseon@kangwon.ac.kr

[1] Present address: *Department of Chemical and Biological Engineering, Korea University, Seoul 136-713, Republic of Korea*

RSC Advances Accepted Manuscript

1. INTRODUCTION

Recently, coated materials have become of great interest because of their importance for fundamental understanding of their properties and also from the point of view of their applications. Bulk materials or particles coated with thin films having desirable electrical, magnetic, mechanical, and optical properties are found to possess excellent new physical properties and can be applied in various fields requiring high-performance materials. For example, the hydrogenated amorphous silicon (a-Si:H) thin films are used for the solar cells, image sensors, electrophotographic drums, thin film transistors, etc.. Although the technology to coat a rather large substrate (in the centimeter range and above) is well established, especially in the microelectronics industry, coating small substrates (smaller than the mm range) is a matter of great importance and difficulty. Coatings can alter the morphology, charge, functionality, and reactivity of the core. The particles can be coated to improve their stability and dispersion characteristics, and also to enhance their chemical and mechanical properties. For example, for catalytic and photocatalytic applications, relatively inexpensive materials such as silica, alumina, and titania with high specific surface areas are coated with more expensive metals or metal oxides which exhibit improved catalytic properties. In this way, the cost of the final products can be substantially reduced [1-7]. A common technology for coating particles involves a wet treatment process. When particles in a dry form are needed for the end use, a wet coating process becomes less attractive because it requires handling of solvents, binders, and surfactants, and involves expensive and complicated process steps such as dispersion, filtration, drying, and waste stream treatment. As an alternative, a dry coating process can also have several advantages such as easy scale-up, high throughput, low costs, and short processing time, depending on particular process [8-10].

To improve physical, and sometimes, chemical properties of particles for various applications, several researchers have coated the thin films on particles by using the gas phase processes. McCormick et al. [5] developed a rotary reactor for atomic layer deposition (ALD) on submicron particles, where ~10 nm Al_2O_3 ALD film was coated onto ZrO_2 particles of average diameter 60 nm. Powell et al. [9,10] introduced the in situ coating of TiO_2 particles (diameter ~1 μm) with SiO_2, Al_2O_3 or Al_2O_3/SiO_2 by chemical vapor deposition, cluster deposition and sintering in a hot wall, continuous flow tubular reactor, and suggested that the precursor concentrations of the coating materials and the reactor temperature could be important variables to control the surface characteristics of the coated particles. Hung et al. [8] used a counter flow diffusion flame reactor to prepare the SiO_2- and Al_2O_3-coated TiO_2 particles (diameter ~50 nm) and investigated the effects of temperature and of Si/Ti and Al/Ti concentration ratios on particle morphologies. Fotou et al. [2] used a continuous flow tubular reactor for preparing the TiO_2 particles (diameter <1 μm) coated with metal oxides (ZrO_2, Al_2O_3/ZrO_2, and SiO_2/ZrO_2), and proposed different film formation mechanisms for these metal oxides with different morphologies. Nakagawa et al. [11] prepared the Cu-fine core particles (diameter ~20 μm) coated with a TiO_2 thin film by using arc-plasmas under an H_2–Ar gas environment and reported the significance of using H_2 in preparing fine composite particles and maintaining a steady state of the arc-plasmas. A vacuum-operated circulating fluidized bed plasma chemical vapor deposition reactor was used to coat the amorphous TiO_2 film on the glass microbeads (diameter ~150 μm) as photocatalysts for water treatment [12] and also to prepare the hard SiC particles coated with the aluminum oxide film to increase the chemical stability of the SiC particles [13]. It was observed that variation of the plasma source from RF to microwave power had no significant influence on the chemical composition of the deposited material. Both the degree of crystallization and the photocatalytic activity were improved by applying thicker TiO_2 films (as compared to thinner films), after UV irradiation-plus-calcining and/or longer calcining [12].

RSC Advances Accepted Manuscript

Chemical vapor deposition (CVD) is now an essential technology for manufacturing semiconductors and other electronic components and for coating substrate materials for wear-resistant tools and for many optical, optoelectronic, and corrosion applications. The CVD involves the formation of a thin solid film on a substrate material by a chemical reaction of vapor-phase precursors. The reaction can be promoted or initiated by heat (thermal CVD), higher frequency radiation such as UV (photo-assisted CVD), or a plasma (plasma-enhanced CVD) [2-5]. Plasma-enhanced CVD (PECVD) is a technique in which electrical energy rather than thermal energy is used to initiate homogeneous reactions for the production of chemically active ions and radicals that can participate in heterogeneous reactions to form a thin layer on the substrate. A major advantage of PECVD over the thermal CVD process is that deposition can occur at low temperature at a reasonable rate, which also allows coating of temperature-sensitive substrates. The temperature of electrons in PECVD can be in the order of 20,000 K or higher, while the temperature of vapor reactants may remain near room temperature. The PECVD utilizes high electron energy to activate the chemical reactions at low temperature [14,15].

Kim et al. [16-22] proposed a rotating PECVD process for uniform particle coating and demonstrated numerically and experimentally that this process can provide a higher quality thin film on particles, as compared with other particle-coating processes. In a rotating cylindrical PECVD reactor, the bars placed at the inside wall of the cylinder lift the particles to the top of cylinder wall, where they fall down to the bottom of cylinder wall (Fig. 1). In this way, one part of the particles is falling through the center of the cylinder, where the bulk plasmas exist, while other part of particles is located on the cylinder wall. For the particles falling through the bulk plasma in the gas phase, their total surface area is available for deposition of precursors for thin films, and the particles will then be coated uniformly with the precursors generated by the plasma reactions. For the particles located on the cylinder wall, only the surface area of the particles that is exposed to the bulk plasma is available for the deposition of precursors, and the upper section of the particles will be coated with the precursors while those particles remain on the cylinder wall.

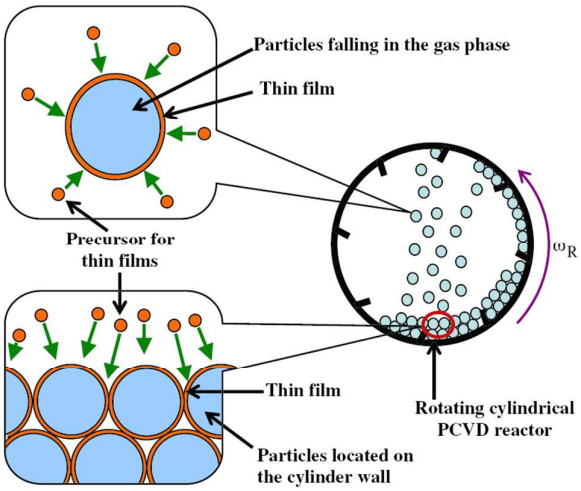

Figure 1. Cross-sectional view of the rotating cylindrical PECVD reactor for particle coating [22].

In this review, we introduce the particle coating technology using a rotating plasma process and the applications of the coated particles. Theoretical and experimental results of this process will be shown, demonstrating the coating of particles of various substrates with TiO_2 and SiO_2 thin films. Several examples of applications of the coated particles for air and water pollution control will also be provided.

RSC Advances Accepted Manuscript

2. THEORETICAL ANALYSIS OF THIN FILM GROWTH

Kim's group calculated numerically the thickness of thin films and growth rate of TiO_2 thin films on the glass beads by a rotating PECVD reactor [16-19]. Calculations were made for TiO_2 thin film deposited onto particles by using titanium tetraisopropoxide (TTIP) as precursor. Fig. 2 shows a schematic of the rotating cylindrical plasma reactor that was used to analyze the particle coating. The inner diameter of the cylinder is 6.5 cm and the distance between two electrodes is 35 cm. Low-temperature plasmas are generated by an inductively coupled rf plasma process with a spiral-shaped electrode installed around the outside wall of the reactor. The plasma reactor rotates with a rotation speed, ω_R, to deposit the chemical species uniformly onto the surface of the glass particles.

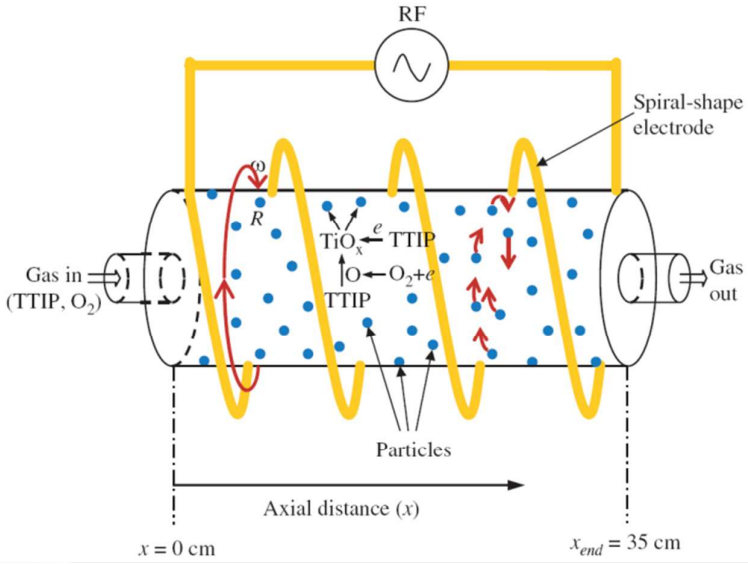

Figure 2. Schematic of the inductively coupled plasma reactor for particle coating [17].

In the TTIP + O_2 plasmas, reactive radicals (O and O('D)) are generated as a result of collisions of highly energetic electrons and O_2 gas molecules. TTIP can be decomposed to generate TiO_x, $Ti(OH)_x$, or $Ti(OH)_x(OR)_{4-x}$ by the electron-impact dissociation reactions and also by the reactions with reactive chemical species, mainly O radicals. TiO_x is the main precursor for thin film on particles, and TiO_x concentration depends on the concentrations of TTIP and O. 9 important plasma reactions were considered for the evolution of TTIP, TiO_x, and O radicals inside the reactor [17]. The number concentrations for chemical species, *i*, in the plasma reactor were calculated from Eqs. (1) and (2) as follows:

$$\frac{dN_i}{dt} = \sum_j^9 \alpha_{ij}(RXN)_j - \nabla(u_s N_i - D\nabla N_i) \qquad (i = 1\text{-}5) \qquad (1)$$

$$\frac{dN_{TiO_x}}{dt} = (k_8 N_e + k_9 N_o) N_{TTIP} - \nabla\left(u_s N_{TiO_x} - D_{TiO_x}\nabla N_{TiO_x}\right) - J_{TiO_x}\left(\frac{2}{R}\right) - J_{TiO_x}\left(\frac{D_P^2}{R^2}\right) N_T W_{FP} \qquad (2)$$

In Eqs. (1) and (2), the first, second, and third terms on the right-hand side represent the effects of plasma chemical reactions, convection, and diffusion, respectively. The fourth and fifth terms in Eq. (2) show the disappearance rates of TiO_x by deposition on the reactor wall and on the particles falling in the gas phase, respectively. N_i, N_{TiOx}, N_e, N_o, and N_{TTIP} are the number concentrations of the *i*th chemical species, TiO_x, electrons, O radicals, and TTIP, respectively. $(RXN)_j$ is the rate of the *j*th reaction, and α_{ij} is the stoichiometric coefficient of the *i*th species in the *j*th reaction. u_s is the gas

RSC Advances Accepted Manuscript

velocity inside the reactor. R, D_P, N_T, D_i and W_{FP} are the reactor radius, particle diameter, number of particles per unit length of the reactor, diffusion coefficients of the chemical species, and fraction of particles falling in the gas phase, respectively [17].

Using model equations, Kim et al. [17] calculated TiO_x, O_2, O radical, and TTIP concentrations and film thickness on the particles along the axial distance. Fig. 3 shows (a) the evolution of the TiO_x concentration profile along the axial distance at t = 10 min, and (b) the change of film thickness on the particles as a function of time at x = 3.6 cm, for various $[TTIP]_0$'s. The initial TTIP partial pressure was changed from 0.005 to 0.02 torr, and the corresponding initial O_2 partial pressure ranged from 0.095 to 0.38 torr at fixed equivalence ratio ($\phi = ([TTIP]_0/[O_2]_0)_{actual}/([TTIP]/[O_2])_{stoichiometric\ ratio}$), ϕ = 0.95. A higher TTIP concentration at the same ϕ causes faster generation of TiO_x and O radicals in the reactor by the plasma reactions, and the TiO_x concentration becomes higher at the reactor inlet and decreases more quickly by faster reaction with O radicals (Fig. 3(a)). Due to faster deposition of TiO_x onto the particles, the TiO_2 film thickness increases more quickly as the initial TTIP partial pressure increases (Fig. 3(b)). The particles with $[TTIP]_0$ = 0.005 and 0.01 torr show almost constant film growth rates for $0 \le t \le 10$ min, but, for $[TTIP]_0$ =0.02 torr, the film growth rate decreases slightly with time.

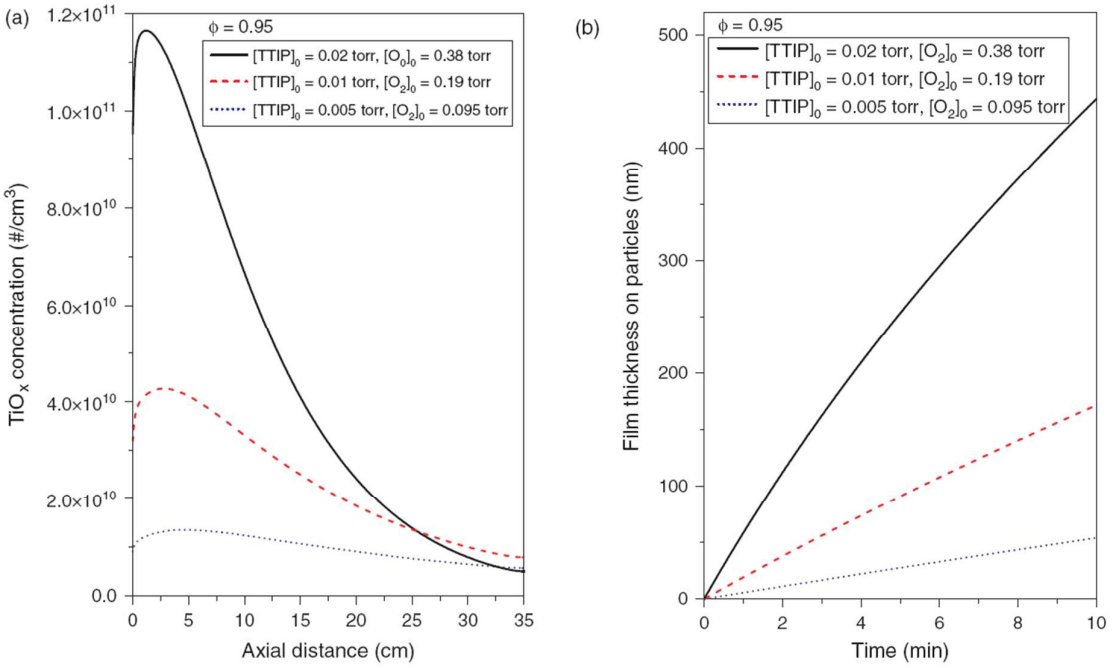

Figure 3. (a) Evolution of TiO_x concentration profile along the axial distance at t = 10 min for various $[TTIP]_0$'s. (b) Change of film thickness on the particles as a function of time at x = 3.6 cm for various $[TTIP]_0$'s [17]

The a-Si:H thin-film growth on particles in the rotating pulsed SiH_4 plasma process was analyzed numerically by Kim et al. [19]. The evolutions of chemical concentrations of SiH_4, SiH_x, SiH^+_x and polymerized negative ions in the pulsed plasmas have been shown during the plasma-on and -off in this research. It was found that, by using the pulsed plasma process, the polymerized negative ions of higher mass can be efficiently reduced and high-quality thin films can be successfully prepared from the deposition of low mass chemical species on the particles. During plasma-on, the SiH_4 concentration decreases as a result of collision reactions with electrons but, during plasma-off,

RSC Advances Accepted Manuscript

increases in the absence of energetic electrons in the plasmas. During plasma-on, SiH_x and SiH^+_x are generated quickly as a result of fast dissociative reaction of SiH_4, but, during plasma-off, SiH_x disappears fast as a result of the reaction with hydrogen and the deposition onto the reactor wall and particles, and SiH^+_x is consumed quickly due to fast neutralization reactions with negative ions. During plasma-on, the concentrations of negative ions increase with time as a result of the polymerization reactions of negative ions, but, during plasma-off, they decrease with time as a result of the neutralization reactions with SiH^+_x.

Fig. 4 illustrates the changes of film thickness on the particles along the axial distance with time. Fig. 4(a) shows that the film thickness on the particles increases with time, as SiH_x deposits onto the particles. The SiH_x concentration in the bulk plasmas is higher than in the sheath regions, and the particles in the bulk plasmas grow more quickly than in the sheath regions by faster deposition of SiH_x onto the particles. In Fig. 4(b), the changes of film thickness on the particles are shown as a function of time for various axial distances in the 1st half of the pulsed plasma reactor ($0 \le x \le 17.5$ cm). During plasma-on, the SiH_x concentration increases quickly and becomes high, in the order of 10^{11} #/cm^3 and the thickness of a-Si:H thin film on the particles increases fast with the deposition of SiH_x, but, during plasma-off, the thin film growth rate decreases quickly and nearly stops, as shown in the subgraph of Fig. 4(b), because the SiH_x concentration decreases quickly and nearly becomes zero [19].

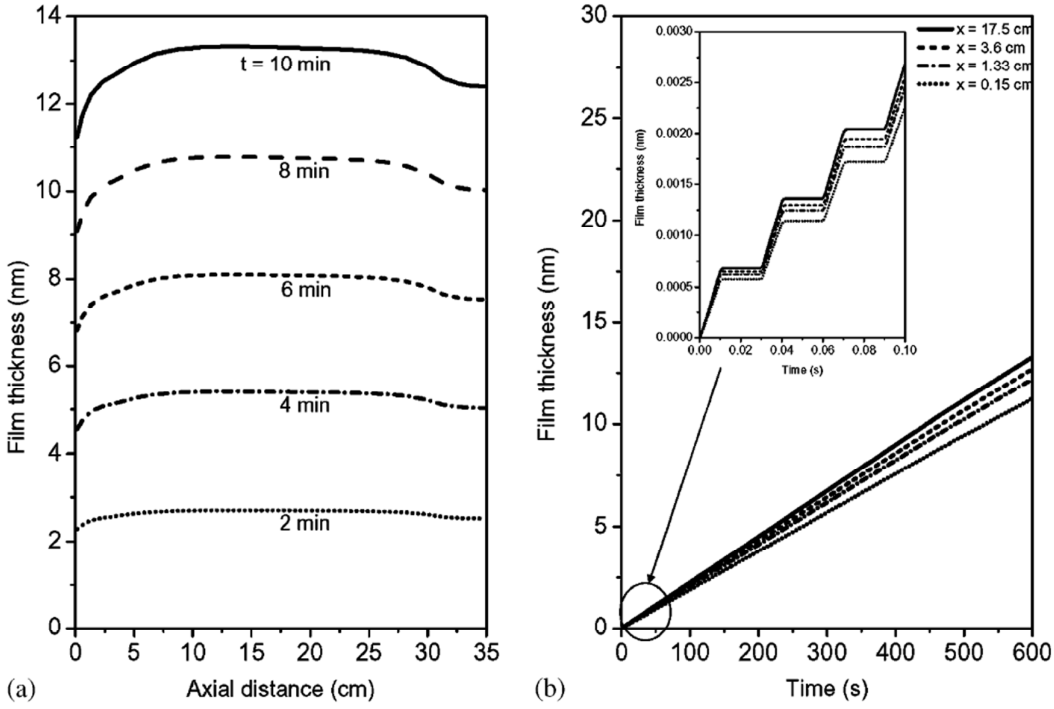

Figure 4. Changes of the film thickness on particles (a) along the axial distance with times, and (b) as a function of time for various axial distances [19].

3. PARTICLE COATING METHODS

3.1. TiO_2 single layer on glass particles

The TiO_2 single layer thin films on glass particles in a rotating cylindrical PECVD reactor were synthesized by Kim's group [20,22]. Fig. 5 shows a schematic of the experimental setup for coating thin films on particles by a rotating PECVD process. Inductively coupled plasmas were generated inside the rotating cylindrical quartz reactor by applying rf power to a spiral-shaped coil electrode, which was located outside the reactor. The rotation speed of the reactor was controlled by using a DC

RSC Advances Accepted Manuscript

motor. N_2 gas was passed through an ultrasonic nebulizer to carry TTIP as a precursor to the reactor. O_2 was supplied to the reactor separately from TTIP to prevent chemical reaction between O_2 and TTIP in the feed line. The flow rates of all gases were controlled precisely by mass flow controllers (MFCs). After coating with TiO_2, the glass particles were treated in a high temperature furnace at 550 ◦C for 2 h [20].

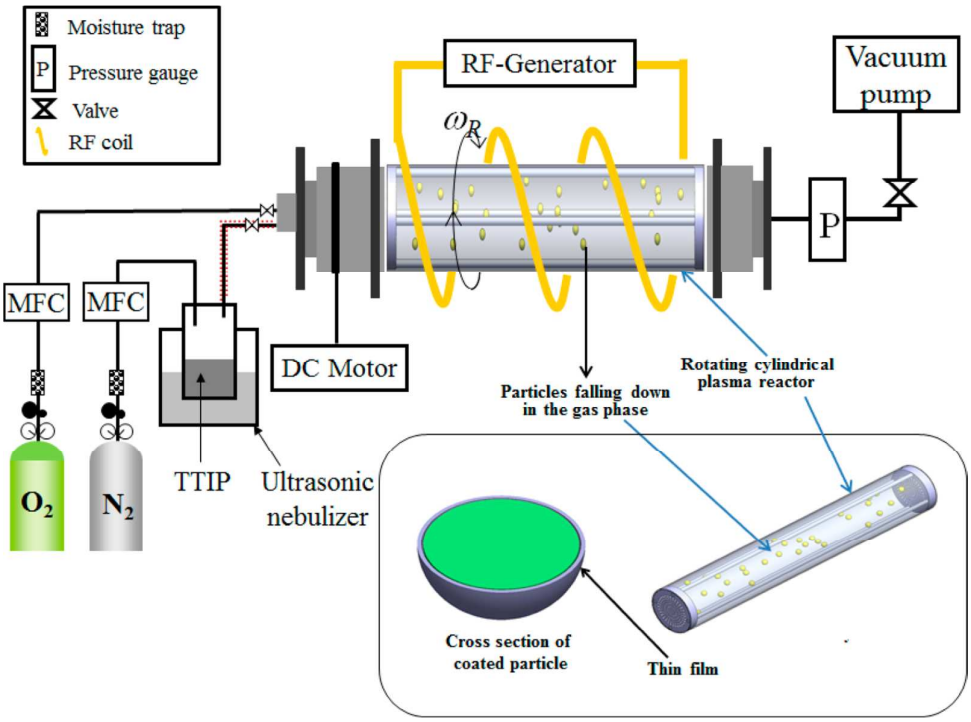

Figure 5. Schematic diagram of the experimental setup for coating glass beads with TiO_2 thin films by the PECVD process [23].

The morphologies and cross-sectional views of the TiO_2 films were analyzed by SEM before and after heat treatment. Particles were mechanically broken in half in order to obtain a cross-sectional view SEM image. Glass particles, especially, were dipped into liquid nitrogen prior to the breaking process in order to make it easier. Several SEM images of thin films coated on the glass beads (diameter 3 mm) were made for different process conditions and the film thicknesses on the glass beads were obtained from the SEM images for each process condition [20]. The SEM images in Fig. 6 show that TiO_2 was deposited on the surface of the glass particles as grains, which were piled up close to each other, making a quite dense coating. The weight of the TiO_2-coated glass particles was measured before and after heat treatment. The TiO_2 thin films appeared to be thinner and denser after a heat treatment due to a decrease of voids inside the thin films and also through loss of carbon and hydrogen compounds from the thin film [20,22].

RSC Advances Accepted Manuscript

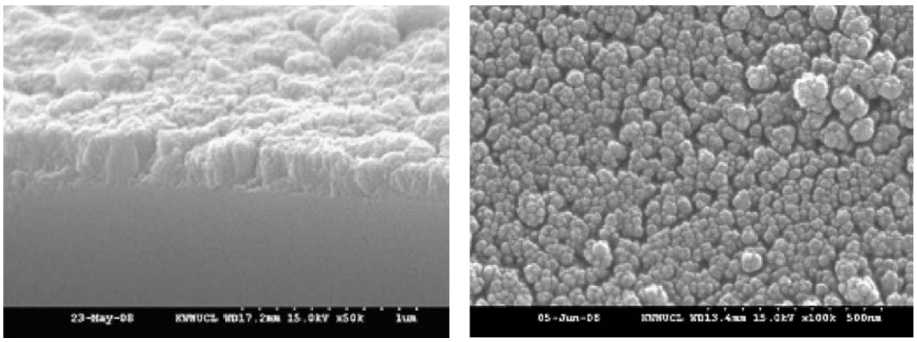

(a) (b)

Figure 6. TiO_2 coating on glass particles: (a) cross-section view; (b) surface of TiO_2 thin film coated on glass particle [20,22].

In the rotating PECVD process, the film thickness can be easily controlled by changing process variables such as precursor flow rate, applied electric power, reactor pressure, rotation speed, number of particles loaded in the reactor, etc.. Fig. 7 shows the thickness of the TiO_2 thin films before and after heat treatment for various mass flow rates of TTIP (a) and various reactor pressures (b). For the TTIP mass flow rates of 1.333, 2.667, and 3.333 mg/min, the film thicknesses are about 99, 216, and 281 nm, respectively, after 1 h of heat treatment (500 °C). The particles grow by the deposition of precursors for the thin films and the increase of particle volume can be expressed by the deposition rates of precursors onto the particles located on the cylinder wall and also onto the particles falling in the gas phase. Since the concentration of precursors for deposition is almost proportional to the TTIP concentration, the thickness of the TiO_2 thin film on the glass beads increases as the mass flow rate of TTIP increases, as shown in Fig. 7. The generation and disappearance rates of precursors for deposition are complicated functions of reactor pressure and, as the reactor pressure increases, the growth rate of the TiO_2 thin film increases, but is not proportional to the reactor pressure [22].

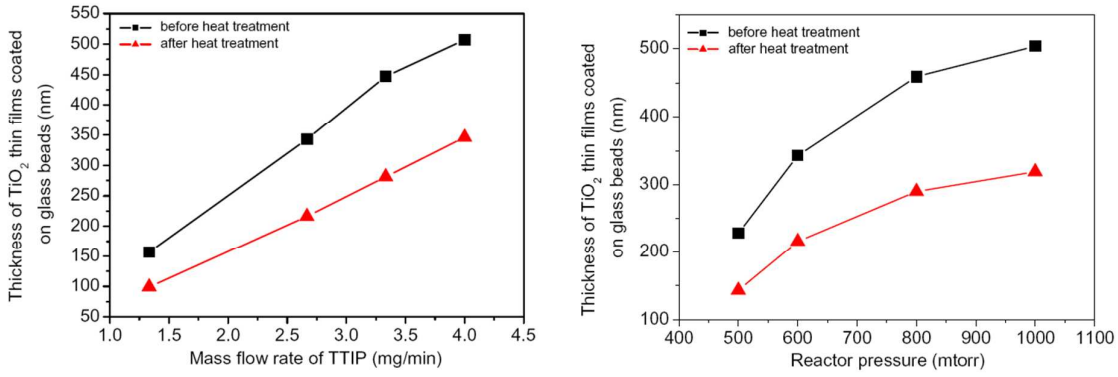

(a) (b)

Figure 7. Thickness of TiO_2 thin film before and after heat treatment for various mass flow rates of TTIP (a) and various reactor pressures (b) [22].

3.2. SiO_x and TiO_y single layer on PP particles

Polypropylene (PP) particles were also used as a substrate for coating SiO_x or TiO_y single-layer film by a rotating PECVD process. SiO_x or TiO_y thin films were coated onto PP particles of 3 mm in diameter by using TEOS (tetraethyl orthosilicate) and TTIP as precursors, respectively. After deposition, the SiO_x or TiO_y thin films on the PP particles were annealed in a N_2 stream at 120 °C for

RSC Advances Accepted Manuscript

2 h. The surface and cross-sectional views of the SiO_x or TiO_y films were analyzed by SEM and EDX [21,24]. Fig. 8 shows the SEM image (a) and EDX data (b) of the cross-section of the SiO_x single-layer films coated onto the PP beads. The SiO_x layer on PP was found to be quite uniform, without particle contamination. The EDX results show that the thin films on the PP beads consist of the O (66.28%) and Si (33.72%) elements, based on weight percentage. The prepared SiO_x was found to be $SiO_{1.72}$ from the EDX results.

Fig. 9 shows the SEM image (a) and EDX data (b) of the cross-section of the TiO_y single-layer films on the PP beads. The thickness of the TiO_y single layer increased with an increase of deposition time. Figure 9(b) shows the EDX results for the TiO_y thin films, which indicates that the TiO_y films consist of the O (39.85%) and Ti (60.15%) elements, based on weight percentage. The TiO_y was found to be TiO_2 from the EDX results [21]. Unlabelled peaks in Figs. 8(b) and 9(b) indicate C and H, which originate from PP as the substrate material.

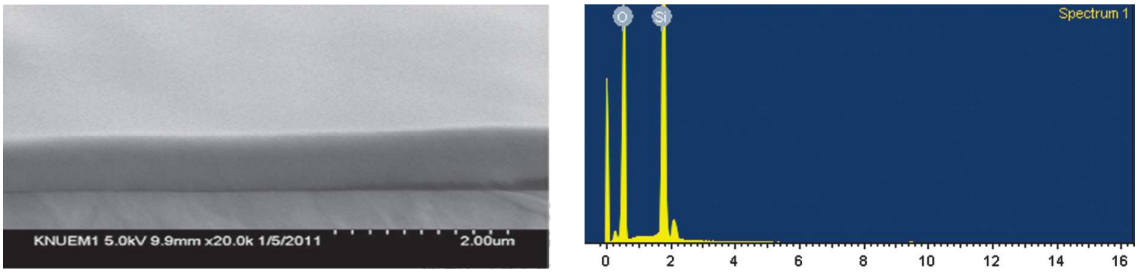

(a) (b)

Figure 8. (a) SEM image and (b) EDX of the cross-section of SiO_x single-layer film on PP bead [21].

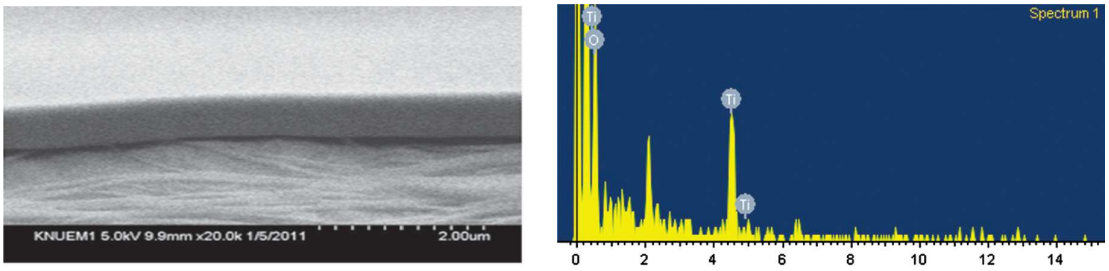

(a) (b)

Figure 9. (a) SEM image and (b) EDX of the cross-section of TiO_y single-layer film on PP bead [21].

3.3. TiO_2/SiO_x double layer coated on glass particles

The photocatalytic activity of TiO_2/SiO_x double-layer films can be enhanced in the double-layer structure, as compared with the TiO_2 single layer due to the presence of SiO_x bottom layer. The SiO_x thin films may act as a trap for the electrons generated in the TiO_2 layer, thus preventing the electron–hole recombinations. Kim's group [24] coated TiO_2/SiO_x double layer films onto glass particles via rotating cylindrical PECVD. The SiO_x bottom layer was first deposited on the glass beads by supplying TEOS into the reactor. Before the deposition of the TiO_y top layer, the SiO_x single-layer films on the glass beads were annealed in N_2 atmosphere at 550 ºC for 2 h. The TiO_y top layer was deposited on the SiO_x bottom layer by supplying TTIP through an ultrasonic nebulizer with N_2 carrier gas. The TiO_y/SiO_x double-layer films on the glass beads were annealed in an O_2 atmosphere at 550 ºC for 2 h and the TiO_y top layer was fully oxidized to provide a TiO_2/SiO_x double-layer film. The SEM image (Fig. 10) of the cross-section of the TiO_2/SiO_x double-layer films on the glass beads clearly shows two separate layers of SiO_x (bottom) and TiO_2 (top).

RSC Advances Accepted Manuscript

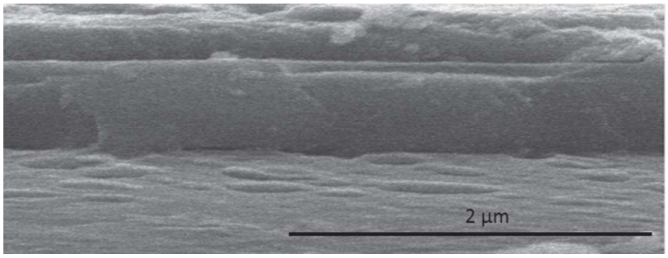

Figure 10. SEM images of the cross-section of TiO_2/SiO_x double-layer films on the glass beads [24].

4. APPLICATIONS OF PARTICLES COATED BY A ROTATING PECVD REACTOR

Particles coated with different kinds of thin films can be utilized in various fields. The application of TiO_2-based photocatalysts is quite attractive for the air and water pollutant removals [25-31], VOCs decomposition [32-34], water splitting [35,36], etc., because of their high activity, stability, and availability for photodegradation. One way to improve the photodegradation efficiency of a TiO_2 photocatalyst is to use small particles coated with TiO_2 thin films, because the surface area of the TiO_2 photocatalyst becomes far larger, as compared with that of a plate substrate coated with TiO_2 thin films. The rotating PECVD process is an efficient method for uniform coating of TiO_2 thin films on the surface of particles to obtain the photodegradation with high efficiency. For example, glass particles and zeolite particles which are dielectric materials, can be used for air pollutant removal in a dielectric barrier discharge process and the TiO_2 photocatalyst coated on such dielectric particles can make the removal process more efficient.

4.1. Application of TiO_2-coated particles obtained by using a rotating PECVD reactor to air pollutant removal

The removal of pollutants such as NO and SO_2 created by industrial processes or contained in vehicle exhausts is important for environmental pollution control, and the dielectric barrier discharge process is one of the methods applicable for air pollutant removal. The removal efficiencies for those pollutants can be improved by the hybridization of the dielectric barrier discharge and photocatalyst process. Fig. 11 shows the experimental setup for removing NO and SO_2 by means of a dielectric barrier discharge-photocatalyst hybrid (DBD-PH) reactor. Glass particles were coated with a uniform thin film of TiO_2 photocatalyst using a rotating PECVD reactor. The glass particles as a dielectric material were packed compactly inside the DBD-PH reactor. A copper rod wire is located at the center of the glass tube, which has the inner and outer diameters of 27 mm and 30 mm, respectively. The outside wall of the reactor is wrapped over by a stainless steel mesh which acts as a ground electrode. The dielectric barrier discharge is generated by applying high voltage power into the reactor and the NO and SO_2 are removed by the plasma reactions [23,37]. The TiO_2 photocatalyst can be activated by the UV light from the plasma discharge, and the removal efficiencies for NO and SO_2 can be enhanced by the photocatalytic reactions.

RSC Advances Accepted Manuscript

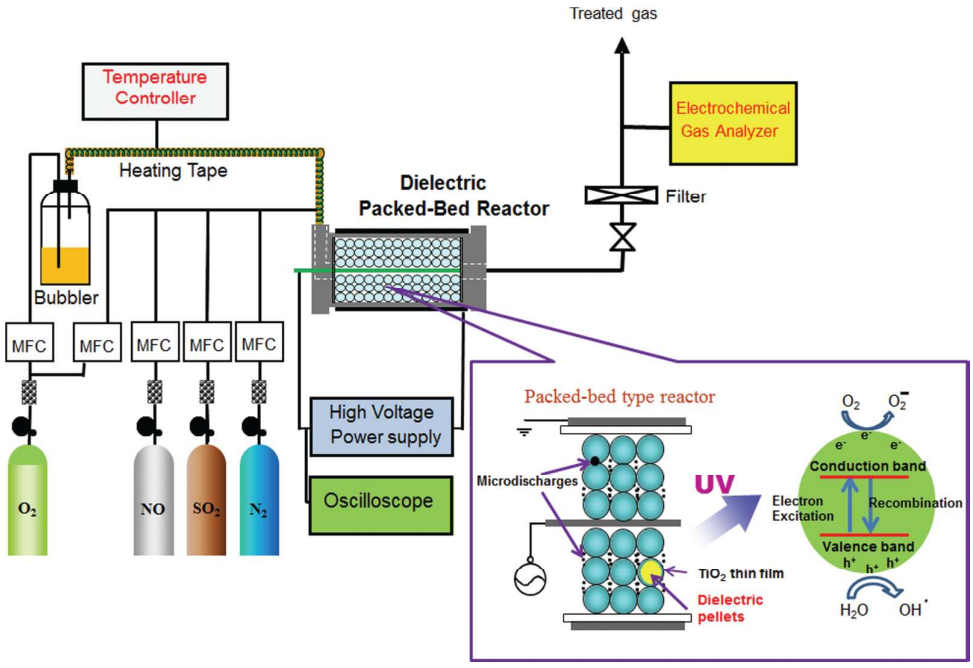

Figure 11. Experimental setup for NO and SO_2 removals by a dielectric barrier discharge-TiO_2 photocatalyst hybrid process [24].

Figs. 12 (a) and (b) show the removal efficiencies for NO and SO_2, respectively, for various thicknesses of TiO_2 thin film as a function of applied peak voltage. The higher applied voltage enhances the generation of reactive radicals (O, N, OH, H, etc.), because of the faster electron-impact dissociation reaction to generate those radicals, and results in the higher removal efficiencies for NO and SO_2 because of their faster oxidation reactions with the reactive radicals. Fig. 12 also shows that the removal efficiencies for NO and SO_2 increase with TiO_2 thickness until the latter reaches 600 nm and then decrease when the TiO_2 thickness increases further. These results indicate that there is an optimum thickness of TiO_2 thin film on glass beads to maximize the NO and SO_2 removal efficiencies by the DBD-PH process [23].

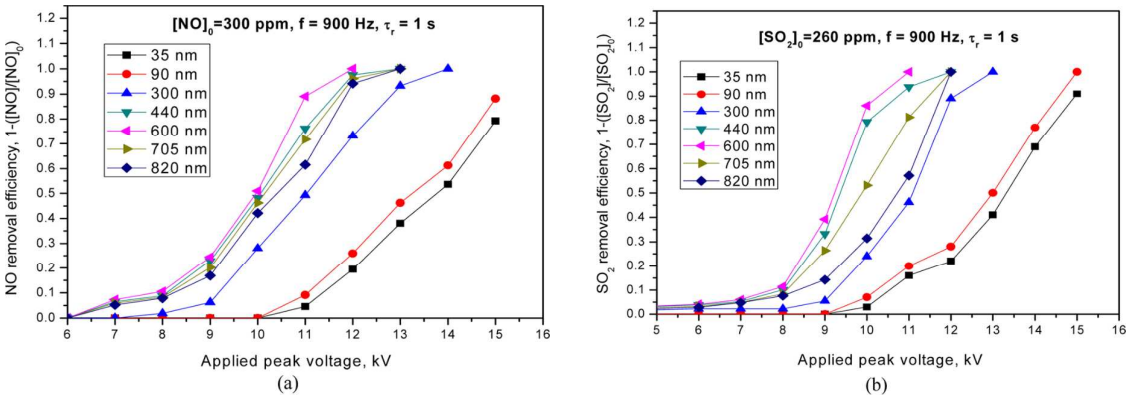

Figure 12 (a) NO and (b) SO_2 removal efficiencies for various thicknesses of TiO_2 thin films as a function of applied peak voltage [23].

Another dielectric material used for air pollutant removal in the DBD-PH process is zeolite catalyst. When zeolite particles (diameter 1.4-2.36 mm) are coated with TiO_2 photocatalyst by this

RSC Advances Accepted Manuscript

rotating PECVD, the NO and SO_2 removal efficiencies can be affected by three combined effects: plasma effect, catalysis, and photocatalysis. Figs. 13 shows the SEM images of the cross section of the zeolite particles (a) before TiO_2 coating and (b) after TiO_2 coating by rotating PECVD for 30 min. Zeolite is a porous material with large surface area. Fig. 13(b) shows that TiO_2 is deposited partially on the surface of the zeolite particles but that the TiO_2 does not cover the whole surface of the zeolite; thus, it does not block all the zeolite pores and the large surface area of the zeolite is preserved. The PECVD process allows easy control of the quantity of TiO_2 deposited onto the zeolite surface by changing the process condition of deposition time [26].

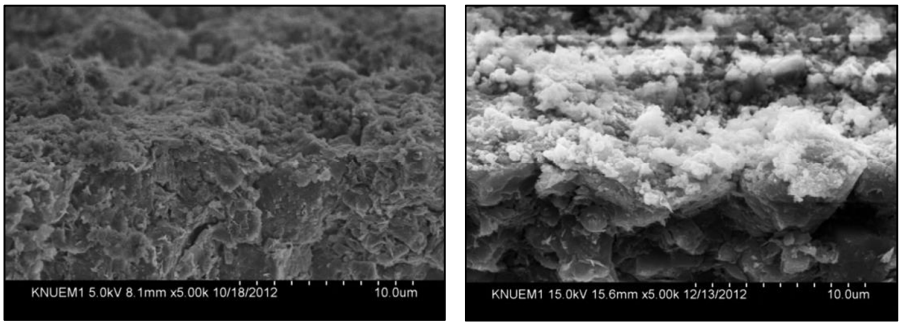

(a) (b)

Figure 13. SEM images of the cross section of the zeolite particles: (a) before coating and (b) after TiO_2 coating for 30 min [26].

Fig. 14 shows the NO and SO_2 removal efficiencies, respectively, by the dielectric barrier discharge-catalyst (DBD-C) hybrid process with zeolite particles and by the dielectric barrier discharge-catalyst-photocatalyst (DBD-C-P) hybrid processes, also with zeolite particles, for various residence times as a function of applied peak voltage. The zeolite particles as a dielectric material were coated with TiO_2 thin film by a rotating PECVD process and were packed inside the DBD-C-P reactor. As the residence time increases for both the DBD-C and DBD-C-P hybrid processes, the NO and SO_2 have more time available for chemical reactions inside the reactor, and the removal efficiencies for NO and SO_2 increase. For a residence time of 2 s, the maximum removal efficiencies of NO and SO_2 become 73% and 100%, respectively, at an applied voltage of 15 kV. The NO and SO_2 removal efficiencies in the DBD-C-P hybrid process here for various residence times are 1.04–3.4 times and 1.02–3.5 times higher, respectively, than those in the DBD-C process [26].

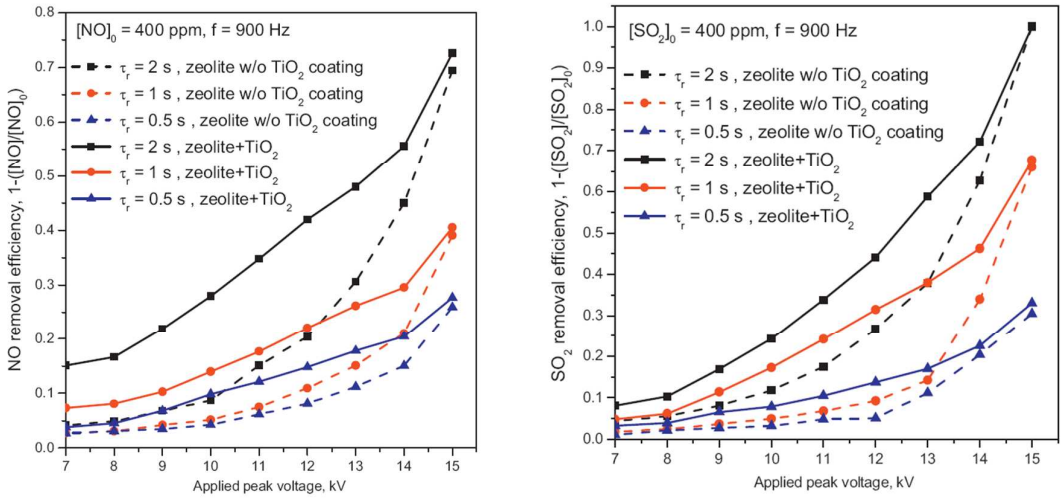

RSC Advances Accepted Manuscript

Figure 14. Comparison of NO and SO_2 removal efficiencies by the DBD-C and DBD-C-P hybrid processes for various residence times as a function of applied peak voltage [26].

4.2. Application of TiO_2-coated particles obtained by using a rotating PECVD reactor to water pollutant removal

Another example of the use of TiO_2-coated particles is the photodegradation of water pollutants. The PP particles coated with TiO_2 thin film by the rotating PECVD process were applied for the photodegradation of phenol in aqueous solution by Kim et al. [38]. Photodegradation experiments on phenol using TiO_2-coated PP particles were carried out in a slurry-type batch reactor holding 300 ml of an aqueous solution of phenol (Fig. 15). The TiO_2-coated PP particles were suspended in the aqueous solution, which was stirred continuously by a magnetic stirrer. O_2 was continuously bubbled into the reactor for all experiments. The UV lamp (wavelength < 365 nm, 1100 μW/cm^2) was placed in the center of the batch reactor to illuminate the phenol solution. The phenol concentration in the solution was measured by means of a UV–VIS spectrophotometer. It was found that the TiO_2 film was deposited on the PP beads strongly and did not peel off during the experiments.

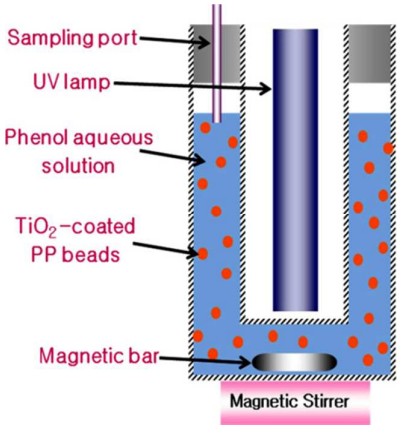

Figure 15. Schematic diagram of the experimental setup for photodegradation of phenol by TiO_2 thin film coated on polypropylene beads [38].

Fig. 16(a) shows the changes of phenol concentration with time for various initial phenol concentrations. As the initial phenol concentration increases, the degradation rate of phenol becomes higher; for an initial phenol concentration of 100 ppm, more than 90% of the phenol was decomposed in 60 min by the TiO_2 thin films coated on the PP beads. Fig. 16(b) shows the changes of phenol concentration for various numbers of PP beads suspended in the aqueous solution. The rate of phenol decomposition is increased by increasing the number of PP beads, because the total surface area of photocatalyst available for photodegradation then increases. The uniform and compact coating of TiO_2 thin films on the PP beads was achieved by means of the rotating cylindrical PECVD reactor. There was no void in the uniform TiO_2 thin films, and O_2 and H_2O could not penetrate through the thin films to reach the PP beads. There was no serious photodegradation of the PP beads observed at the interface of the TiO_2 thin film and the PP beads for the long-term use of these photocatalysts [38].

RSC Advances Accepted Manuscript

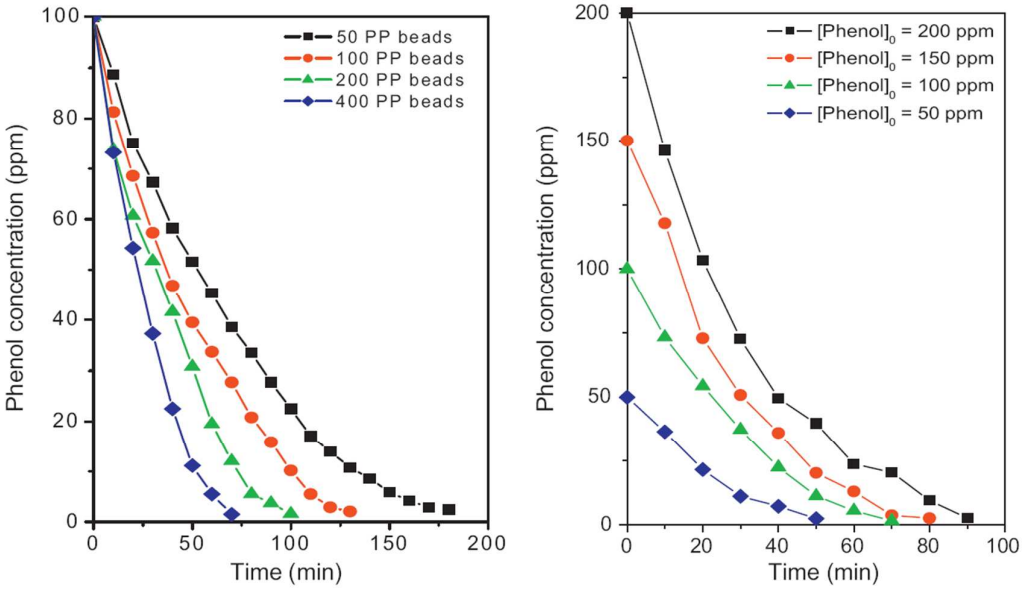

Figure 16. Changes of phenol concentration (a) for various initial phenol concentrations and (b) for various numbers of polypropylene beads coated with TiO_2 thin film [38].

5. CONCLUSION

This review has presented a current development of rotating PECVD process for particle coating, as well as several applications of coated particles produced thereby. The data reported in this review demonstrates that the rotating PECVD reactor can be utilize in order to prepare the high-quality uniform thin films on particles. By changing various process variables such as deposition time, precursor feed rate, reactor pressure, number of particles, applied power, and rotation speed of the reactor, we can accurately control the thickness of the thin films deposited on the particles. The potential application of this process to a large variety of substrate shapes and thin film materials makes this process attractive for many applications such as water and air pollutant removals, VOCs decomposition and water splitting, etc. The rotating PECVD process can also be used to prepare the high-functional particles coated with metal or organic thin films for the enhanced stability and dispersion characteristics, as well as improved chemical and mechanical properties.

Acknowledgements

This work was supported by the Regional Innovation Center for Environmental Technology of Thermal Plasma (ETTP) at Inha University, designated by the Ministry of Trade, Industry and Energy, Republic of Korea. This study was also supported by Kangwon National University.

REFERENCES

1. Papp, J., Shen, H. S., Keshaw, R., Dwight, K., and Wold, A.. Titanium (IV) Oxide Photocatalysts with Palladium, *Chem. Mater.* 5, **1993**, 284–288.
2. Fotou, G.P.; Kodas, T.T.; Anderson, B. Coating Titania Aerosol Particles with ZrO_2, Al_2O_3/ZrO_2, and SiO_2/ZrO_2 in a Gas-phase Process. *Aerosol Sci. Tech.* **2000**, 33, 557-571.

RSC Advances Accepted Manuscript

3. Koga, K.; Kai, M.; Shiratani, M.; Watanabe, Y.; Shikatani, N. Cluster Suppressed Plasma Chemical Vapor Deposition Method for High Quality Hydrogenated Amorphous Silicon Films. *Jpn. J. Appl. Phys*. **2002**, 41(2), 168-170.
4. Koga, K.; Kaguchi, N.; Shiratani, M.; Watanabe, Y. Correlation Between Volume Fraction of Clusters Incorporated into a-Si:H Films and Hydrogen Content Associated with Si–H_2 Bonds in the Films. *J. Vac. Sci. Technol., A* **2004**, 22(4), 1536-1539.
5. McCormick J. A., Cloutier B. L., Weimer A. W., George S. M. Rotary reactor for atomic layer deposition on large quantities of nanoparticles. *J. Vac. Sci. Technol. A*. **2007**, 25(1), 67-74.
6. Taga, Y. Recent Progress of Nanotechnologies of Thin Films for Industrial Applications. *Mater. Sci. Eng., C* **2001**, 15, 231–235.
7. Zhang, L.; Ranade, M.B.; Gentrya, J.W. Formation of Organic Coating on Ultrafine Silver Particles Using a Gas-phase Process. *J. Aerosol Sci.* **2004**, 35, 457-471.
8. Hung, C.-H.; Miquel, P.F.; Katz, J.L.; Formation of Mixed Oxide Powders in Flames: Part II. SiO_2–GeO_2. *J. Mater. Res.* **1992**, 7, 1870-1875.
9. Powell, Q.H.; Fotou, G.P.; Kodas, T.T.; Anderson, B.M.; Guo, Y. Gas Phase Coating of TiO_2 with SiO_2 in a Continuous Flow Hot-Wall Aerosol Reactor. *J. Mater. Res.* **1997**, 12, 552-559.
10. Powell, Q.H.; Fotou, G.P.; Kodas, T.T.; Anderson, B.M. Synthesis of Alumina- and Alumina/Silica-Coated Titania Particles in an Aerosol Flow Reactor. *Chem. Mater.* **1997**, 9, 685-693.
11. Nakagawa, T.; Hieda, M.; Shindo, D.; Saito, F.; Yubuta, K.; Nishimura, K.; Fujii, T. Preparation of a Fine Powder Composed of Oxide–Metal Composite by an Arc-Plasma Method. *Powder Technol.* **2003**, 130, 456-461.
12. Karches, M.; Morstein, M.; Rudolf von Rohr, P.; Pozzo, R.L.; Giombi, J.L.; Baltanás, M.A. Plasma-CVD-Coated Glass Beads as Photocatalyst for Water Decontamination. *Catal. Today* **2002**, 72, 267-279.
13. Karches, M.; Morstein, M.; Rudolf von Rohr, P.; Encapsulation of Abrasive Particles by Plasma CVD. *Surf. Coat. Technol.* **2003**, 169–170, 544-548.
14. Chemical Vapor Deposition, Anthony C. Jones, Michael L. Hitchman, Royal Society of Chemistry, 2009.
15. Handbook of Chemical Vapor Deposition: Principles, Technology, and Applications, Hugh O. Pierson, William Andrew Publishing, LLC, 2nd Edition, 1999..
16. Kim, K.S.; Kim D.J. Analysis on Uniform Particle Coating by the Rotating Cylindrical PCVD Reactor, *J. Aerosol Sci*. **2006**, 37(11), 1532-1544.
17. Kim D.-J.; Baeg J.-O.; Moon S.-J.; Kim K.-S. Uniform Coating of TiO_2 Thin Films on Particles by Rotating Cylindrical PCVD Reactor, *J. Nanosci. Nanotechnol*. **2009**, 9(7), 4285-4292.
18. Kim D.-J.; Kim K.-S. Prediction of TiO_2 Thin Film Growth on the Glass Beads in a Rotating PCVD Reactor, *J. Nanosci. Nanotechnol* **2010**, 10(5), 3211-3215.
19. Kim K.-S.; Kim D.-J.; Zhao Q.Q. Numerical Analysis on Particle Coating by the Pulsed Plasma Process, *Chem. Eng. Sci*. **2006**, 61, 3278-3289.
20. Kim D.-J.; Kang J.-Y.; Kim K.-S. Preparation of TiO_2 thin films on glass beads by a rotating plasma reactor, *J. Ind. Eng. Chem*. **2010**, 16(6), 997-1000.
21. Pham H.C.; Kim K.-S. Thin Film Coating of Particles through the plasma process, *J. Nanoelectron. Optoe.* **2011**, 6(3), 264-267.
22. Kim D.-J.; Kang J.-Y., Kim K.-S. Coating of TiO_2 Thin Film on Particles by Plasma Chemical Vapor Deposition Process, *Adv. Powder Technol*. **2010**, 21, 136-140.

RSC Advances Accepted Manuscript

23. Pham H.C.; Kim K.-S. Effect of TiO_2 Thin Film Thickness on NO and SO_2 Removals by Dielectric Barrier Discharge-Photocatalyst Hybrid Process, *Ind. Eng. Chem. Res*. **2013**, 52(15), 5296-5301.
24. Pham H.C.; Kim K.-S. Preparation of TiO_2/SiO_x Double-Layer Films on Glass Beads and Its Application to NO and SO_2 Removal, *J. Nanosci. Nanotechnol.* **2012**, 13(8), 5568-5571.
25. Kim D.-J.; Pham H.C.; Kim K.-S. Application of PCVD Process to Uniform Coating of TiO_2 Thin Films on Polypropylene Beads, *Surface Review and Letters*, 17(3), 2010, 329-335.
26. Nasonova A.; Kim K.-S. Effects of TiO_2 Coating on Zeolite Particles for NO and SO_2 Removal by Dielectric Barrier Discharge Process, *Catal. Today*, **2013**, 211, 90-95.
27. Nasonova A.; Pham H.C.; Kim D.-J.; Kim W.-S.; Charinpanitkul T.; Kim K.-S. Application of TiO_2-Coated Alumina Beads to Dielectric Barrier Discharge-Photocatalyst Hybrid Process for NO and SO_2 Removals, *J. Nanosci. Nanotechnol*. **2011**, 11(2), 1323-1327.
28. Chang M.B.; Balbach J.H.; Rood M.J.; Kushner M.J. Removal of SO_2 from Gas Streams Using a Dielectric Barrier Discharge and Combined Plasma Photolysis. *J. Appl. Phys.* **1991**, 69(8), 4409-4417.
29. Hoffmann M.R.; Martin S.T.; Choi W.; Bahnemann D.W. Environmental Applications of Semiconductor Photocatalysis. *Chem. Rev*. **1995**, 95, 69–96.
30. Mills A.; Davies R.H.; Worsley D. Water Purification by Semiconductor Photocatalysis. *Chem. Soc. Rev.* **1993**, 22, 417-425.
31. Matthews R.W. Photooxidation of Organic Impurities in Water Using Thin Films of Titanium Dioxide. *J. Phys. Chem*. **1987**, 91, 3328–3333.
32. Lee B.-Y.; Park S.-H.; Lee S.-C.; Kang M.; Choung S.-J. Decomposition of Benzene by Using a Discharge Plasma–Photocatalyst Hybrid System, *Catal. Today* **2004,** 93–95, 769–776.
33. Stafford U.; Gray K.A.; Kamat P.V. Photocatalytic Degradation of Organic Contaminants: Halophenols and Related Compounds. *Heterogen. Chem. Rev*. **1996**, 3, 77–104.
34. Ogata A.; Einaga H.; Kabashima H.; Futamura S.; Kushiyama S.; Kim H.H. Effective Combination of Nonthermal Plasma and Catalysts for Decomposition of Benzene in Air. *Appl. Catal. B: Environ.*, **2003**, 46, 87-95.
35. Kudo A., Photocatalyst Materials for Water Splitting, *Catalysis Surveys from Asia*, **2003** 7(1), 31-38.
36. Meng N.; Michael K.H.; Leung, D.; Leung, Y.C.; Sumathy K., A Review and Recent Developments in Photocatalytic Water-Splitting Using TiO_2 for Hydrogen Production, *Renew. Sust. Energ. Rev*. **2007**, 11, 401–425.
37. Nasonova A.; Cuong P.H.; Kim D.-J.; Kim K.-S. NO and SO_2 Removal in Non-Thermal Plasma Reactor Packed with Glass Beads-TiO_2 Thin Film Coated by PCVD Process, *Chem. Eng. J.* **2010**, 156(3), 557-561.
38. Kim D.-J.; Pham H.C.; Park D.-W.; Kim K.-S. Preparation of TiO_2 Thin Films on Polypropylene Particles by a Rotating PCVD Process and Its Application to Organic Pollutant Removal, *Chem. Eng. J.* **2011**, 167(1), 308-313.

RSC Advances Accepted Manuscript